Available online at www.sciencedirect.com
ScienceDirect
Advances in Space Research 44 (2009) 926–933
ADVANCES IN SPACE RESEARCH (a COSPAR publication)
www.elsevier.com/locate/asr

# Extension of INCL4 between 2 and 15 GeV

S. Pedoux [a,*], J. Cugnon [a], A. Boudard [b], J.-C. David [b], S. Leray [b]

[a] University of Liège, AGO Dep., IFPA, Allée du 6 Août 17, bât B5a, B-4000 Liège, Belgium
[b] SPhN/Irfu, CEA-Saclay, F-91191 Gif-sur-Yvette Cedex, France

Received 26 November 2008; received in revised form 6 April 2009; accepted 6 April 2009

**Abstract**

The intranuclear cascade model INCL4 has been shown to be very successful for describing, without adjustable parameters, a whole set of data for p-induced reactions in the 40 MeV–2 GeV energy range. In view of its possible application to cosmic ray interactions, the INCL4 code has been extended to the 2–15 GeV energy range, so covering a large part of the spectrum of the incident energy of the cosmic rays.

In this paper, the changes brought into the INCL4 code are discussed and some illustrative comparisons between the results given by the modified version of the code and experimental data are presented.


*Keywords:* Simulation code; Monte-Carlo; Cosmic rays; Nuclear reactions; Spallation

## 1. Introduction

The research on possible transmutation of nuclear waste has led to the improvement of intranuclear cascade evaporation models over the last years. The Liege intranuclear cascade model (INCL4) has proven to be one of the most performing models when coupled with the ABLA evaporation-fission code developed by Gaimard and Schmidt (1991). It reproduces a whole bunch of experimental data in the 40 MeV–2 GeV range (Boudard et al., 2002) including total reaction cross-sections, particle multiplicities, double-differential cross-sections, residue mass spectra, isotopic distributions and recoil energy spectra.

The cosmic ray particles undergo the same type of nuclear reactions as described by INCL4 when they interact with matter. The analysis of the cosmic ray energy spectrum reveals that the proton flux is maximum around 1 GeV and decreases rapidly as energy increases (Longair, 1997). Therefore, if INCL4 could accommodate a projectile with a kinetic energy up to ~15 GeV, it could potentially be an interesting tool for the simulation of radiation effects.

Of course, to completely describe cosmic rays, INCL4 should be able to accommodate heavy ions as well because they are responsible for high ionization damages. This improvement of the code is also under development and we are not going to discuss it further, concentrating here our attention on proton–nucleus collisions in the 2–15 GeV energy range.

Many other intranuclear cascade models for nucleon–nucleus interaction exist: BERTINI (Bertini, 1963), ISABEL (Yariv and Fraenkel, 1979), FLUKA (Ballerini et al., 26), CASCADE (Barashenkov and Kumawat, 2004), CEM (Mashnik et al., 2005) and even others which are directly included in particle transport codes. It is not the place here to make a thorough comparison between these models. We want just to mention that INCL4 views the target as a collection of nucleons (in contrast with a continuum as supposed in ISABEL), adopts a collision criterion based on a minimum distance of approach, and in the energy range mentioned has no free parameter. Even the time at which the cascade is stopped is determined self-consistently (see Boudard et al. (2002)), avoiding the coupling to a pre-equilibrium stage as in the CEM model.

* Corresponding author. Tel.: +32 43663644; fax: +32 43663672.
*E-mail addresses:* spedoux@ulg.ac.be (S. Pedoux), cugnon@plasma.theo.phys.ulg.ac.be (S. Leray).

0273-1177/$36.00 © 2009 COSPAR. Published by Elsevier Ltd. All rights reserved.
doi:10.1016/j.asr.2009.04.009

In Section 2 we briefly present the standard INCL4 model and we give some insight on the collision mechanisms, the key to the extension of the code. We explain in Section 3 the modifications that have been implemented in the numerical code. Finally, we display in Section 4 a comparison between simulations from the modified version of the code and experimental data at incident energies comprised between 2 and 15 GeV.

## 2. The Liege intranuclear cascade model

The spallation reactions were first described by Serber (1947). Based on the analysis of neutron energy spectra, he assumed that spallation reactions could be described by two different stages:

(1) the intranuclear cascade, the fastest part of the reaction,
(2) the deexcitation of the nucleus.

As indicated by its name, INCL4 describes only the first of these processes. It is a time-like simulation code, based on Monte-Carlo methods. A complete description of the INCL4 model can be found in the article of Boudard et al. (2002).

The main features of the model are illustrated in Fig. 1 which represents fairly well the way INCL4 simulates a reaction. The code begins by randomly generating a target nucleus, all nucleons are given a position and a momentum according to Saxon-Woods and Fermi Sphere distributions, respectively. The projectile is also generated and all particles are propagated. When two particles reach their minimum distance of approach ($d_{\min}$ in Fig. 1), they may interact. All the considered interactions are binary and the interaction criterion can be formulated as: two particles interact when their impact parameter squared and multiplied by $\pi$ is smaller than the total interaction cross-section of these particles. The Pauli principle is applied and can forbid the collision when the phase-space in the vicinity of the potential final states is already occupied. If an interaction takes place, the numerical code determines, using Monte-Carlo methods, whether the collision is elastic or not, and selects the final channel according to the respective cross-sections.

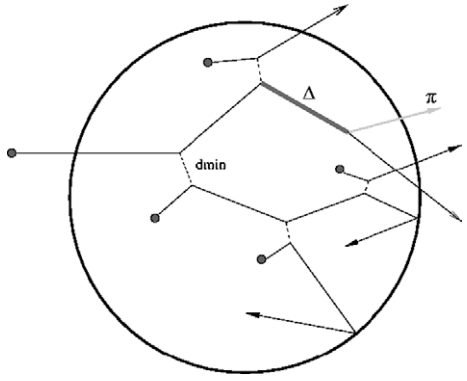


Fig. 1. Example of intranuclear cascade simulated by INCL. Possible reactions visible on this figure are elastic collision, inelastic collision with Δ production, Δ decay, transmission and reflection on nucleus surface.

In the standard version of INCL4, inelastic nucleon–nucleon collisions produce a Δ resonance. This approximation is quite reasonable because, below 2 GeV, the Δ resonance, which is very broad, dominates all other channels. The Δ particle is given a life-time, at the end of which it can decay into a pion and a nucleon. Particles inside the nucleus may also interact with its surface, possibly being reflected or transmitted, as it is shown in Fig. 1.

The chain of reactions and collisions in the nucleus develops until a time $t_{\text{stop}}$, the stopping time, which is an important parameter. At the end of the intranuclear cascade INCL4 is coupled with an evaporation code to simulate the second step of the spallation reactions. INCL4 has the advantage that it does not have any free parameter to run, not even $t_{\text{stop}}$, which is self-determined by the code.

In any binary collision, energy and momentum are conserved, but angular momentum is not conserved. The consequences of this non-conservation is investigated in Cugnon et al. (1997), where a sophisticated procedure is adopted in order to almost conserve angular momentum: it is shown that in the GeV range, the results for the most important observables are practically similar to those with the ordinary procedure.

The time-ordering of the binary collisions is automatically given by the initial conditions. In practice, pairs of particles are checked to see at what time they are going to reach their minimum relative distance and whether this minimum distance is small enough to allow a collision. A table of possible colliding pairs $a, b$ and corresponding collision times $t_{ab}$ is so built. The first collision corresponds to the smallest of these times. When the collision is realized, the table is updated and the next smallest time is selected, and so on. It should be noted that this time-ordering breaks relativistic invariance. Calculations made in different frames yield different results. It is shown however in Cugnon et al. (1981) that results in Lorentz frames "bracketed" by the target and the projectile frames, i.e. frames with positive velocity with respect to the target and a negative velocity with respect to the projectile, differ from each other by a few per cent.

## 3. The extension of the model

The extension of INCL4 mostly consists in adding, for nucleon–nucleon collisions, the new inelastic channels that open in the 2–15 GeV energy range. The major part of them corresponds to the production of non-strange resonances. There are a lot of them and they are strongly overlapping. Furthermore, they have short life-time and decay mainly by pion emission. Hence, we tried a simpler and different procedure than the implementation in INCL4 of all these resonance productions and decays in nucleon–nucleon collisions: we preferred to implement direct

multiple pion production (referred as multipion production) without going through the resonance step. We also identified two other types of reactions to be added to the code:

- Inelastic channels in pion–nucleon collisions ($\pi$–$N$).
- Production of strange particles

The inelastic $\pi$–$N$ collisions have now been implemented in the code but not the strange particle production. These latter channels should account for 10% of the total inelastic cross-sections, in the energy range of interest, and it is our purpose to include them in the code.

The total nucleon–nucleon inelastic cross-sections can then be viewed as the sum of all the different inelastic cross-sections corresponding to all pion producing channels. Therefore the extension of INCL4 requires the search and the parametrization of the cross-sections of the new channels:

- Multipion production: $\sigma(NN \rightarrow a\pi NN)$ with $a = 1,\ 2,\ 3$ or 4.
- $\pi$–$N$ inelastic channels: $\sigma(\pi N \rightarrow \pi\pi NN)$.
- Strange particle production.

The direct parametrization of cross-sections for every channel is not always possible. Quite often, data are imprecise or missing. It is possible to minimize the number of parametrized cross-sections by taking advantage of the isospin symmetry. Such a procedure is explained in the article of Bystricky et al. (1987). Following this procedure, we computed generic $\sigma_T(NN \rightarrow a\pi NN)$ with $a = 1, 2, 3$ or 4 and $T = 0, 1$, the third isospin component of the system formed by the two colliding nucleons. Those generic cross-sections are obtained as linear combinations of particular channel cross-sections. The extra benefit of the procedure lies in the fact that the number of parametrized particular cross-sections needed to obtain $\sigma_T(NN \rightarrow a\pi NN)$ is smaller than the total number of particular cross-sections. As an example, in the three pion production case, the procedure reduces of 50% the number of needed parametrized cross-sections.

In the four pion production case, the linear combination is not unique any more and the procedure cannot be applied. In the 2–15 GeV energy range, the channels producing more than 4 pions remain negligible, thus we fixed:

$$\sigma_T(NN \rightarrow 4\pi NN) = \sigma_{T,\mathrm{Inel}} - \sigma_T(NN \rightarrow \pi NN) - \sigma_T(NN \rightarrow 2\pi NN) - \sigma_T(NN \rightarrow 3\pi NN) \quad (1)$$

Once the number of produced pions is selected, the electric charges of the outgoing particles have to be determined. We proposed a model based on isospin symmetry and Clebsch–Gordan coefficients to associate a probability with each charge repartition, allowing the code to fix the charges of the particles with Monte-Carlo methods. This probability is a function of the isospin state of the produced pions and the incoming and outgoing nucleons. The isospin state of a system of 4 pions cannot be univoquely computed, that is why the model was adapted for the 4 pion production channels. We assumed that 4 pion production channels are similar to 2 pion production channels with two additional pions being either $\pi^+\pi^-$ or $\pi^0\pi^0$. Hence, we assumed that the probabilities associated with 4 pion production channels are the same as 2 pion production channels multiplied by a factor which represents the multiplicities of the two additional pions.

The determination of momenta and energies of the outgoing particles also requires a new specific model, since the standard version of INCL4 handles only two outgoing particles in nucleon–nucleon interactions. The model we used is based on the FOUL subroutine of James (1977) from CERN libraries. It randomly generates the momenta and the energies in a phase-space with uniform density.

The $\pi$–$N$ inelastic channels were added to the code using the same procedures as for multipion production channels. We used the procedure of Bystricky et al. (1987) to compute the generic cross-section $\sigma_T(\pi N \rightarrow \pi\pi N)$ where $T = \frac{1}{2}, \frac{3}{2}$ is the third isospin component of the system formed by the pion and the nucleon. We also used the model based on Clebsch–Gordan coefficients and isospin symmetry for the charge repartition and the same model as above for the energy and momentum repartition.

## 4. Comparison with experimental data

After the implementation of the multipion production reactions in N–N collisions and of the inelastic reactions in $\pi$–$N$ collisions, we made calculations in order to check whether our assumptions were reasonable. The shortcut, consisting by simply replacing excitation and decay of resonances by direct production of pions, is tested by direct comparison with experimental data. As shown below, these tests reveal to be promising.

Fig. 2 shows, on the top (bottom) panel, a comparison for total positive (negative) pion yield between experimental data coming from Collot et al. (2000) and simulations given by the modified version of INCL4. The shapes of the symbols refer to the target nucleus and are explained in the figures. Filled symbols refer to the simulations and empty symbols refer to the experimental data, when available, for the same nucleus.

As we can see, the agreement between simulations and data is encouraging, even though one can notice that the simulation results are systematically 10% higher than the data. This can be explained by the fact that the strange particles production has not been introduced in the code yet and the addition of these channels will diminish the amount of inelastic cross-sections in N–N collisions presently devoted to multipion production. We can expect that the implementation of these channels will mitigate the present overestimate of total pion yield. Experimental indications as well as theoretical arguments are pointing indeed

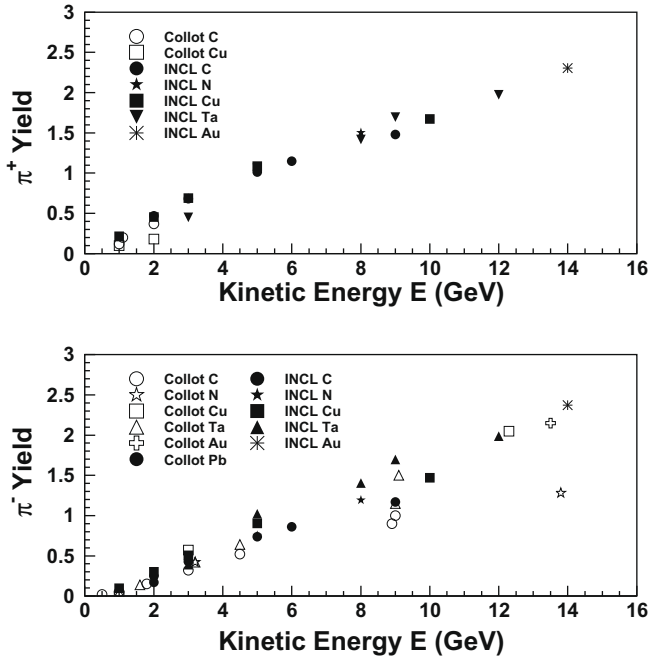


Fig. 2. Positive (negative) pion total yield on the top (bottom) panel with respect to the kinetic energy of the projectile in various proton–nucleus interactions.

toward a strange particle yield being of the order of 10% of the pion yield in the energy range under consideration (Wong, 1994).

The left (right) panel in the Fig. 3 shows a comparison between measured and simulated cross-section for the $\pi^+(\pi^-)$ production as a function of the target mass number. The experimental data come from the HARP Collaboration (2007a,b,c). They refer to positive and negative pion

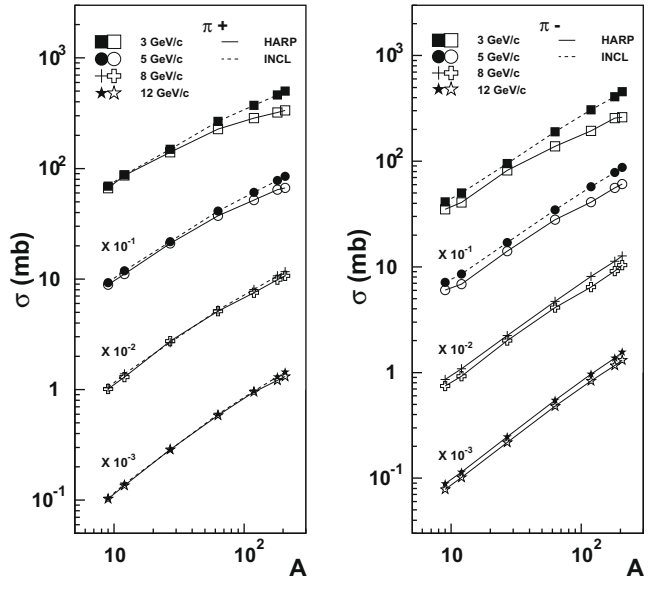


Fig. 3. Positive (negative) pion production integrated cross-section on the left (right) panel with respect to the mass number A of the target nucleus at four different kinetic energies of the projectile. See text for details.

inclusive cross-sections for protons with 3, 5, 8 or 12 GeV/c momentum and beryllium, carbon, aluminium, copper, tin, tantalum or lead targets. The different proton momenta are represented by a different symbol. It can be seen in Fig. 3 that the dependance of the total pion production on the mass number of the target is close to a power law.

The experimental results of the HARP Collaboration provide double-differential cross-sections for $\pi^+$ and $\pi^-$ production. Cross-sections quoted in Fig. 3 are obtained by integrating double-differential cross-sections over the momentum and angular domain covered by the HARP experiment. The latter extends from 350 to 2150 mrad for emission angle and from 100 to 800 MeV/c for pion momentum. We can see in the figures that the overall agreement is satisfying but, as the target mass increases, the simulations grow more distant with the experimental measurements.

We limited ourselves to show, in this paper, a detailed comparison between simulated $\pi^+$ production double-differential cross-sections and measured ones for only one target. We choose lead as the target nucleus. The discrepancy being the largest at high mass number, this case may be helpful for tracing back the origin of this discrepancy. The double-differential cross-sections, with their experimental errors, are displayed in Figs. 4–7 as a function of the pion momentum. The numbers stand for the four momenta of the incident particles, which are indicated on the top of each figure.

Globally the model that we have introduced, namely the replacement of all nucleon resonances by direct pion production, seems to work correctly. The agreement between simulations and experimental data is generally better for angles bigger than 1 rad and for the low pion momentum region. In Figs. 4 and 5, it seems obvious that the simulations lead to a pion yield bigger than the experimental one. The case for 8 and 12 GeV/c figures is less obvious. The shapes of the simulations and the experimental data are quite different, which lead to the conclusion that a uniform phase-space population may not be a good assumption at high incident energy.

Figs. 8–11 show the simple-differential cross-sections for $\pi^+(\pi^-)$ on the left (right) panels after integration over the momentum for the top panels and after integration over angles for the bottom panels, the integration intervals are indicated on the top right corner of each figure. The experimental errors are not reported in these figures. Some information on the errors for the partially integrated cross-sections can be found in HARP Collaboration (2007a) but not on totally integrated cross-sections. As before, each figure corresponds to a given momentum for the incident proton, which is specified at the top of them.

It appears in these figures that the shape of simulated $d\sigma/d\theta$ are satisfactorily reproduced for all incoming protons momentum, even though it is overestimated in the 3 GeV/c case. The simulated $d\sigma/dp$ for high momentum pions are overestimated for every incoming proton

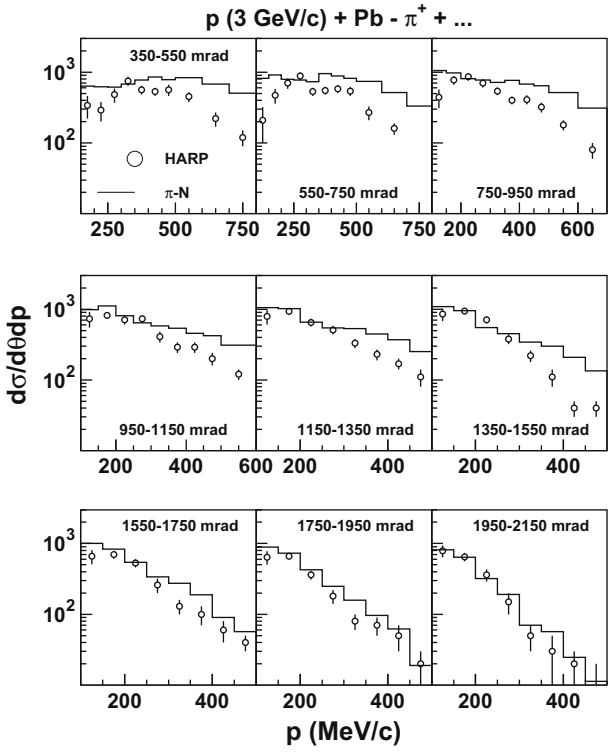


Fig. 4. Double-differential cross-sections for $\pi^+$ production in 3 GeV/c p-Pb interaction as a function of the pion momentum. The angular bins are indicated on the panels.

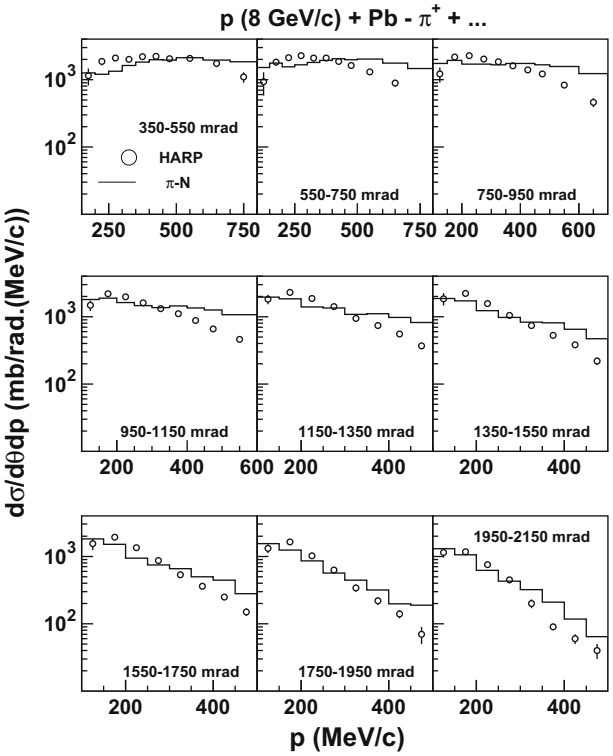


Fig. 6. Double-differential cross-sections for $\pi^+$ production in 8 GeV/c p-Pb interaction as a function of the pion momentum. The angular bins are indicated on the panels.

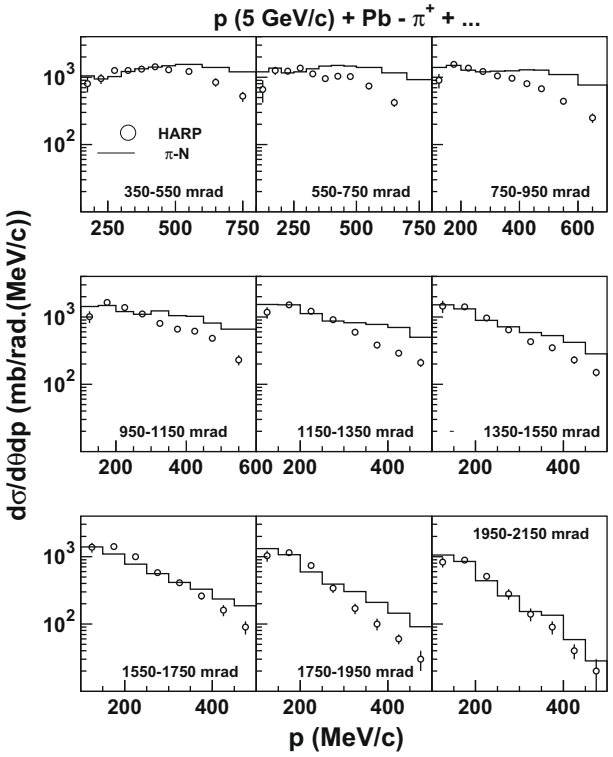


Fig. 5. Double-differential cross-sections for $\pi^+$ production in 5 GeV/c p-Pb interaction as a function of the pion momentum. The angular bins are indicated on the panels.

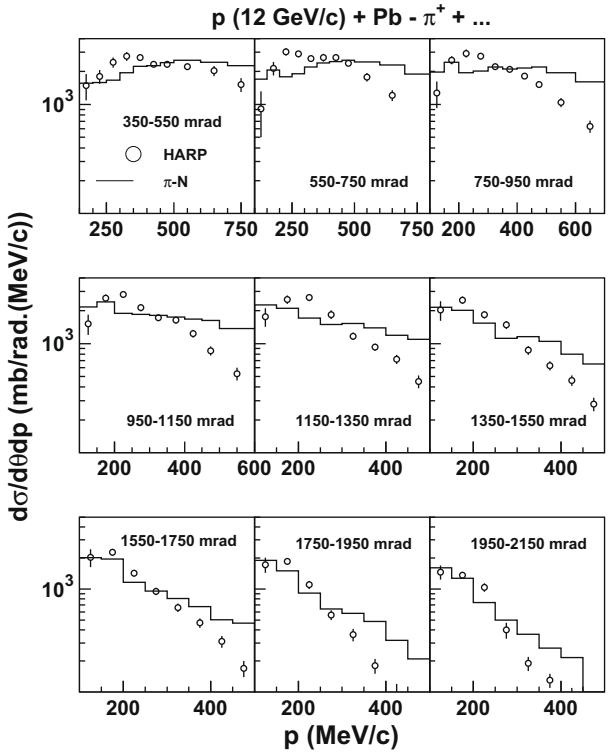


Fig. 7. Double-differential cross-sections for $\pi^+$ production in 12 GeV/c p-Pb interaction as a function of the pion momentum. The angular bins are indicated on the panels.

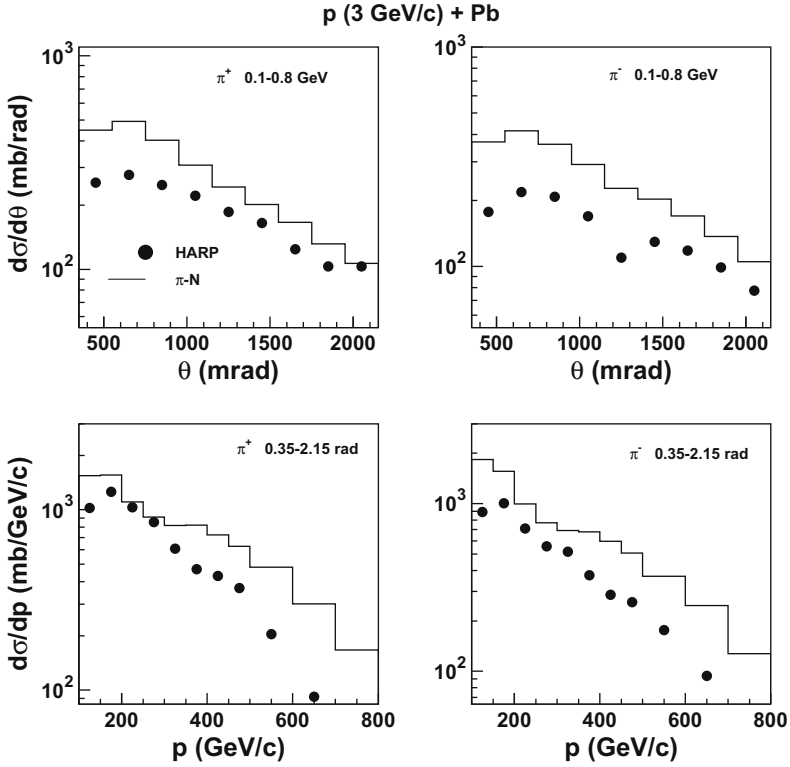


Fig. 8. Simple-differential production cross-sections for $\pi^+$ (two panels on the left) and $\pi^-$ (two panels on the right) in 8 GeV/c p-Pb integrated over momentum (two panels on the top) and over angular region (two panels at the bottom).

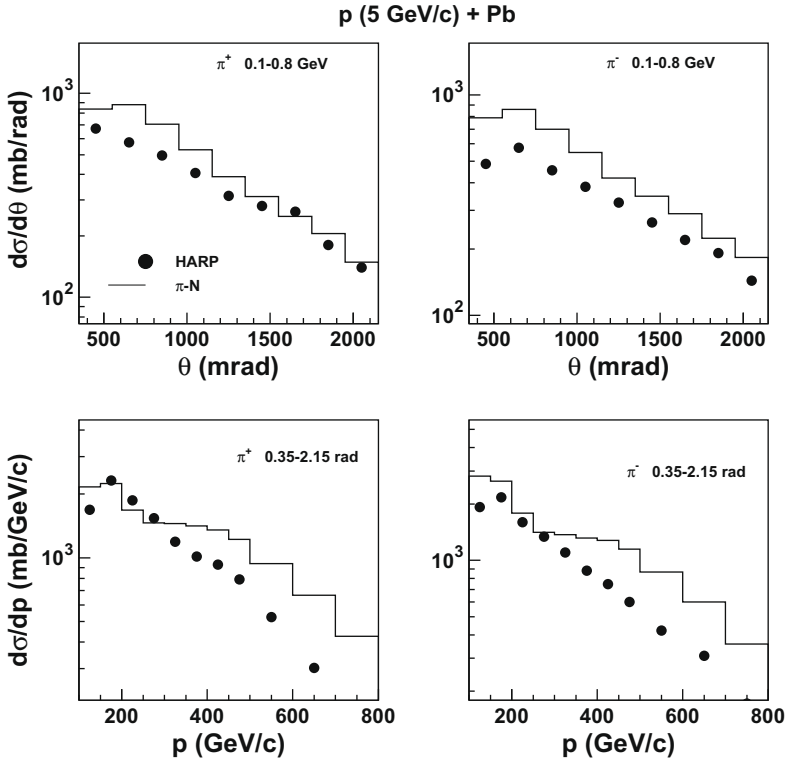


Fig. 9. Simple-differential production cross-sections for $\pi^+$ (two panels on the left) and $\pi^-$ (two panels on the right) in 5 GeV/c p-Pb integrated over momentum (two panels on the top) and over angular region (two bottom panels).

momentum while it is underestimated in the low momentum region for high incoming proton momentum. The discrepancies in the $d\sigma/dp$ shape between simulations and HARP data may indicate that our assumption of a uni-

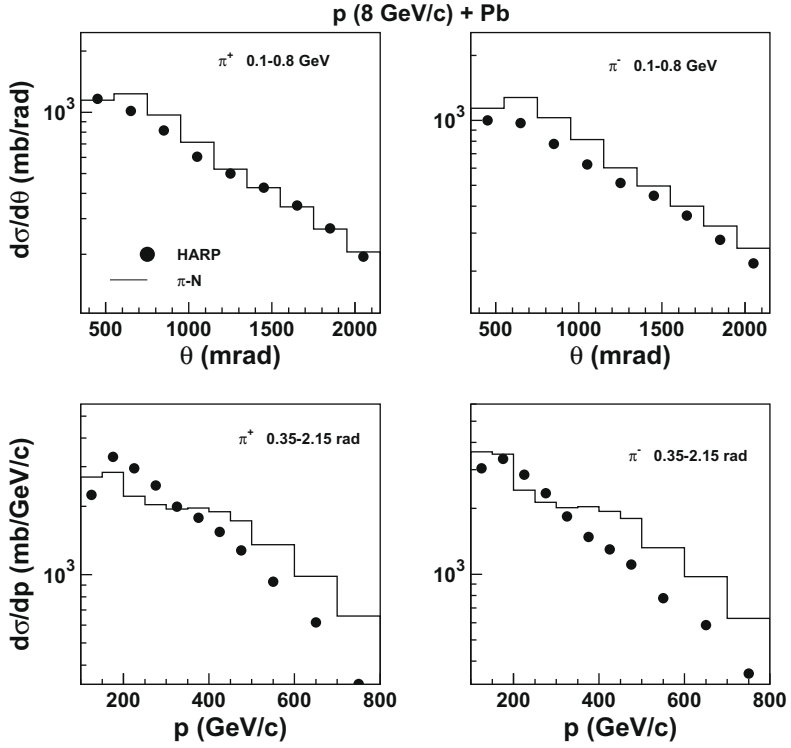


Fig. 10. Simple-differential production cross-sections for $\pi^+$ (two panels on the left) and $\pi^-$ (two panels on the right) in 8 GeV/c p-Pb integrated over momentum (two panels on the top) and over angular region (two bottom panels).

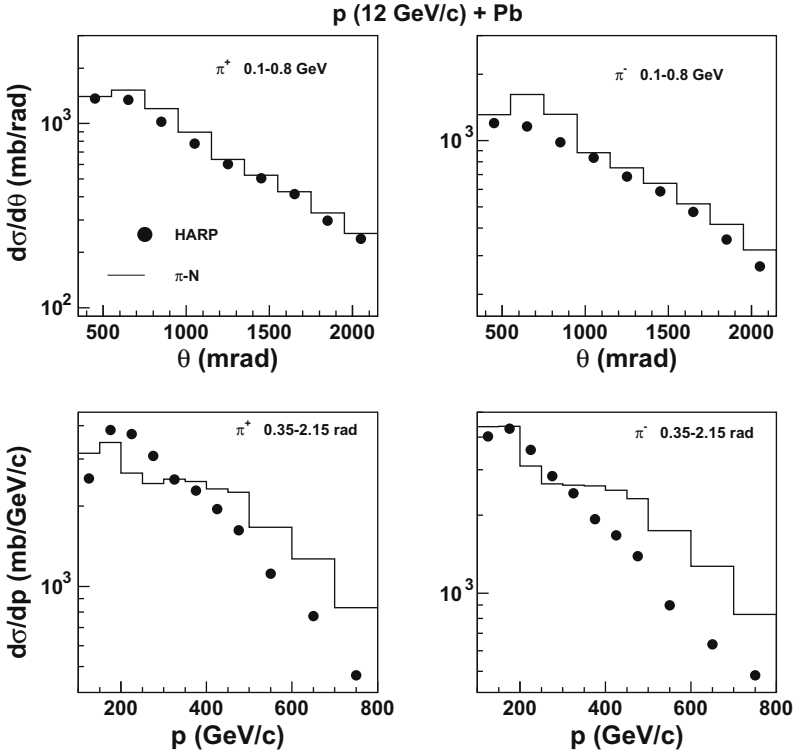


Fig. 11. Simple-differential production cross-sections for $\pi^+$ (two panels on the left) and $\pi^-$ (two panels on the right) in 12 GeV/c p-Pb integrated over momentum (two panels on the top) and over angular region (two bottom panels).

formly populated phase-space is not correct, especially for high momentum incoming protons. Presumably the production of pions is more forward and backward peaked in the center of mass frame than assumed in this model.

We are currently working on this hypothesis. The global overestimation of pion production yield around 3 GeV/c especially for heavy targets (see Fig. 3) is not really sensitive to the detail of the phase-space model. It may indicate that at this low incident momentum, the role of resonances (other than the Δ resonance) is not negligible.

The primary goal of this work is to see whether a description based on direct pion production in nucleon–nucleon interactions is a viable alternative to the usual description in terms of resonances. At this point a comparison with a comparable calculation based on this second picture would be welcomed. The calculation of Nara et al. (1999) provides with a good example. It is based on the JAM hadronic cascade approach. We cannot produce a direct comparison since this numerical code is not available to us. As far as we can judge from the results shown in Nara et al. (1999), especially from Figs. 20 and 22 of their work, our results are of comparable but slightly lesser quality. The interest of our model is that the description of the inelastic processes is much simpler, avoiding the whole machinery of the heavy resonance production, with the accompanying set of largely unknown cross-sections for interaction of these resonances.

## 5. Conclusion

The extension of the intranuclear cascade model of Liège is almost complete. The multipion production channels and inelastic $\pi$–$N$ channels, which have been identified as the major part of channels opening in the 2–15 GeV energy range, have been implemented in the code.

A comparison between experimental data and the predictions of the modified INCL4 has been done and shows promising results. Simulated total pions yields are close to corresponding data, but the introduction of strange particles production could improve it further. The agreement between simulated angular distributions of the produced pions and measured ones is reasonable. The momentum distributions are not completely satisfactorily reproducing high energy reactions and a modification of the phase-space model that we introduced in the code is probably required in order to improve our predictions for these quantities.

## Acknowledgements

This work has been partially done in the frame of the EU IP EUROTRANS project (European Union Contract No. FI6W-CT-2004-516520). We acknowledge the EU financial support. S. Pedoux has benefitted from a IISN (Belgium) fellowship.

## References

Ballerini, F., Battistoni, G., Cerutti, F., et al. Nuclear Models in FLUKA: Present Capabilities, Open Problems and Future Improvements, Presented at ND2004, Santa Fe, 26 September–1 October, 2004, SLAC-PUB-10813 Report, 2004.

Barashenkov, V.S., Kumawat, H. Development of Monte-Carlo Model of High Energy Nuclear Interactions, JINR E11-2004-121 Report, Dubna, 2004.

Bertini, H.W. Low-energy intranuclear cascade calculation. Phys. Rev. 131, 1801–1821, 1963.

Boudard, A., Cugnon, J., Leray, S., Volant, C. Intranuclear cascade model for a comprehensive description of spallation reaction data. Phys. Rev. C 66, 044615, 1–28, 2002.

Bystricky, J., La France, P., Lehar, F., Perrot, F., Siemiarczuk, T., Winternitz, P. Energy dependence of nucleon–nucleon inelastic total cross-sections. J. Phys. 48, 1901–1924, 1987.

Collot, J., Kirk, H.G., Mokhov, N.V. Pion production models and neutrino factories. NIM A 451, 327–330, 2000.

Cugnon, J., Mizutani, T., Vandermeulen, J. Equilibrium in relativistic nuclear collisions. A Monte-Carlo calculation. Phys. Rev. C 22, 505–534, 1981.

Cugnon, J., Volant, C., Vuillier, S. Improved intranuclear cascade model for nucleon–nucleus interactions. Nucl. Phys. A 620, 475–509, 1997.

Gaimard, J.-J., Schmidt, K.-H. A reexamination of the abrasion–ablation model for the description of the nuclear fragmentation reaction. Nucl. Phys. A 531, 709–745, 1991.

HARP Collaboration. Measurement of the Production Cross-section of Charged Pions by Protons on a Tantalum Target. Available from: arXiv:0706.1600v1, 2007.

HARP Collaboration. Large-angle Production of Charged Pions by 3–12.9 GeV/c Protons on Beryllium, Aluminium and Lead Targets. Available from: arXiv:0709.3458v1, 2007.

HARP Collaboration. Large-angle Production of Charged Pions by Protons on Carbon, Copper and Tin Targets. Available from: arXiv:0709.3464v1, 2007.

James, F. FOWL a General Monte-Carlo Phase Space Program. CERN Computer Centre Program Library, 1977.

Longair, M. High Energy Astrophysics. Cambridge University Press, Cambridge, England, 1997.

Mashnik, S.G., Gudima, K.K., Sierk, A.J. Prael, R.E. Improved intranuclear cascade models for the codes CEM2k and LAQGSM, in: AIP Conf. Proc., vol. 769, pp. 1188–1192, 2005.

Nara, Y., Otuka, N., Ohnishi, A., Niita, K., Chiba, S. Relativistic nuclear collisions at 10 A GeV energies from p + Be to Au + Au with the hadronic cascade model. Phys. Rev. C 61, 024901, 1999.

Serber, R. Nuclear reactions at high energies. Phys. Rev. 72, 1114–1115, 1947.

Wong, C.-Y. Introduction to High-energy Heavy-ion Collisions. World Scientific, Singapore, 1994.

Yariv, Y., Fraenkel, Z. Intranuclear cascade calculation of high-energy heavy-ion interactions. Phys. Rev. C 20, 2227–2243, 1979.